salts.

**Registry No.** 1, 57673-31-1; **2a**, 137364-15-9; **2b**, 137364-16-0; **2c**, 137490-29-0.

**Supplementary Material Available:** Tables of anisotropic thermal parameters, calculated hydrogen positional parameters, and complete bond lengths and bond angles and torsion angles (10 pages); a listing of calculated and observed structure factors (14 pages). Ordering information is given on any current masthead page.

# Synthesis and Spectroscopic Investigations of Alkylaluminum Alkoxides Derived from Optically Active Alcohols. The First Structural Identification of an Optically Active Organoaluminum Alkoxide

Michael L. Sierra, Rajesh Kumar, V. Srini J. de Mel, and John P. Oliver*

*Department of Chemistry, Wayne State University, Detroit, Michigan 48202*

*Received February 19, 1991*

The reaction of trialkylaluminum, $R_3Al$ (R = Me, Et, *i*-Bu), with optically active alcohols such as *l*-menthol and *l*-borneol in a 1:1 ratio gives high yields of $R_2AlOR^*$ ($OR^*$ = *l*-mentholate, R = Me (**1a**), Et (**1b**), *i*-Bu (**1c**); $OR^*$ = *l*-borneolate, R = Me (**2a**), Et (**2b**), *i*-Bu (**2c**)) and the corresponding alkane, RH. The resulting alkoxides have been characterized by $^1H$ and $^{13}C$ NMR spectroscopy. The single-crystal X-ray structures of **1a,c** and **2a** established the dimeric structure for these compounds. **1a** was assigned to the orthorhombic cell system, space group $P2_12_12_1$ (No. 19), with cell constants $a$ = 10.097 (1) Å, $b$ = 10.485 (1) Å, $c$ = 26.920 (4) Å, and $Z$ = 4 (dimers). The structure was refined to a final $R$ = 4.5% ($R_w$ = 3.9%) based on 2669 observed reflections ($F_o \geq 2.5\sigma(F)$). **1c** was assigned to the triclinic cell system, space group $P\bar{1}$ (No. 1), with cell constants $a$ = 10.838 (4) Å, $b$ = 12.792 (6) Å, $c$ = 15.787 (7) Å, $\alpha$ = 81.56 (4)°, $\beta$ = 83.04 (4)°, $\gamma$ = 73.01 (3)°, and $Z$ = 2 (dimers). The structure was refined to a final $R$ = 8.7% ($R_w$ = 8.5%) based on 4213 observed reflections ($F_o \geq 3\sigma(F)$). **2a** was assigned to the monoclinic cell system, space group $P2_1$ (No. 4), with cell constants $a$ = 7.261 (7) Å, $b$ = 14.494 (8) Å, $c$ = 12.938 (7) Å, $\beta$ = 93.63 (7)°, and $Z$ = 2 (dimers). The structure was refined to a final $R$ = 5.3% ($R_w$ = 4.4%) based on 1432 observed reflections ($F_o \geq 2.5\sigma(F)$). In **1a,c** and **2a**, the alkoxide ligands serve as bridging units between the two dialkylaluminum moieties to give stable, planar $Al_2O_2$ rings. The behavior of the $^1H$ NMR spectra of **1a–c** as a function of temperature has been interpreted in terms of increasing steric interaction of the *l*-mentholate group with the methyl, ethyl, and isobutyl groups attached to the aluminum. This steric interaction gives rise to restricted rotation of the *l*-mentholate and/or the alkyl group and leads to nonequivalence of the protons in the ethyl and isobutyl derivatives. This does not occur for the *l*-borneol derivatives, since the borneol moiety cannot interact with the alkyl groups bound to the aluminum because of its orientation and rigidity.

## Introduction

During the past several years a great deal of interest has been focused on the use of organometallic compounds in regio- and stereospecific organic synthesis.[1] Increasing emphasis has been placed on the transfer of optical activity from a transition-metal or a main-group-metal center to the substrate. Among the main-group metals studied, the modified aluminum hydride "ate" complexes, incorporating in them an optically active center (e.g., $LiAlH_2(OR)_2$, $LiAlH_2(O_2R)$; R = optically active group), have been found to be very attractive intermediates in enantio- and stereoselective organic syntheses.[2,3] Recently a few optically active organoaluminum compounds such as $EtAl(Cl)OR^*$[4] ($OR^*$ = *l*-mentholate) have been proposed, but never isolated and characterized, as reaction intermediates in the enantioselective ortho hydroxyalkylation of phenols[5] and in asymmetric Diels–Alder reactions.[6] As a part of our investigations of the reactions of alkylaluminum compounds with protic organic substrates,[7] we report the synthesis and detailed spectroscopic investigations of optically active organoaluminum alkoxides derived from *l*-menthol and *l*-borneol and the first structural characterization of optically active organoaluminum alkoxides $[Me_2Al(\mu\text{-}l\text{-mentholate})]_2$, $[(i\text{-Bu})_2Al(\mu\text{-}l\text{-mentholate})]_2$, and $[Me_2Al(\mu\text{-}l\text{-borneolate})]_2$. We have also studied the temperature dependence of the $^1H$ NMR spectra of these derivatives and have determined that in the *l*-menthol derivatives hindered rotation occurs as a result of steric interaction between the menthol group and the alkyl substituents bound to the aluminum atom.

## Experimental Section

**General Data.** All solvents were purified and dried by standard techniques.[8] Argon gas was purified by passing the argon through a series of columns containing Deox catalyst (Alfa), phosphorus pentoxide, and calcium sulfate. Aluminum alkyls

(1) Maruoka, K.; Banno, H.; Yamamoto, H. *J. Am. Chem. Soc.* **1990**, *112*, 7791 and references therein.
(2) Yamamoto, K.; Fukushima, H.; Nakazaki, M. *J. Chem. Soc., Chem. Commun.* **1984**, 1490.
(3) Noyori, R.; Tomino, I.; Tanimoto, Y.; Nishizawa, M. *J. Am. Chem. Soc.* **1984**, *106*, 6709.
(4) Hayakawa, Y.; Fueno, T.; Furukawa, J. *J. Polym. Sci., Part A-1* **1967**, *5*, 2099.
(5) Bigi, F.; Casiraghi, G.; Casnati, G.; Sartori, G.; Zetta, L. *J. Chem. Soc., Chem. Commun.* **1983**, 1210.
(6) Hashimoto, S.-I.; Komeshima, N.; Koga, K. *J. Chem. Soc., Chem. Commun.* **1979**, 437.
(7) Oliver, J. P.; Kumar, R. *Polyhedron* **1990**, *9*, 409.
(8) Shriver, D. F. *The Manipulation of Air-Sensitive Compounds*; McGraw-Hill: New York, 1969.

0276-7333/92/2311-0206$03.00/0 

**Table I. $^1$H NMR Chemical Shifts of the -AlR$_2$ Moiety ($\delta$ in ppm; $J$ in Hz) in $C_6D_6$**

| compd | alkyl α-CH | alkyl β-CH | alkyl γ-CH |
|---|---|---|---|
| $Me_3Al$ | −0.32 (s, 9 H) | | |
| $Et_3Al$ | 0.32 (q, $^3J$ = 9, 6 H) | 1.10 (t, $^3J$ = 9, 9 H) | |
| $(i\text{-Bu})_3Al$ | 0.24 (d, $^3J$ = 6, 6 H) | 1.91 (m, 3 H) | 0.97 (d, $^3J$ = 6, 18 H) |
| **1a** | −0.42 (s, 6 H) | | |
| **1b** | 0.20 (m, 4 H) | 1.32 (t, $^3J$ = 9, 6 H) | |
| **1c** | 0.26 (dd, $^2J$ = 14, $^3J$ = 8, 2 H)<br>0.18 (dd, $^2J$ = 14, $^3J$ = 8, 2 H) | 2.05 (m, 2 H) | 1.13 (d, $^3J$ = 6, 6 H)<br>1.11 (d, $^3J$ = 6, 6 H) |
| **2a** | −0.42 (s, 6 H) | | |
| **2b** | 0.23 (q, $^3J$ = 9, 4 H) | 1.28 (t, $^3J$ = 9, 6 H) | |
| **2c** | 0.28 (d, $^3J$ = 6, 4 H) | 2.04 (m, 2 H) | 1.17 (d, $^3J$ = 6, 12 H) |

(Aldrich; 2.0 M $Me_3Al$ solution in toluene, 1.9 M $Et_3Al$ solution in toluene, and 1.0 M $(i\text{-Bu})_3Al$ solution in toluene), *l*-menthol (Aldrich), and *l*-borneol (Aldrich) were used as received. All glassware used in the synthetic work was oven-dried. The compounds are both oxygen- and water-sensitive, so standard Schlenk-line techniques were employed. Optical rotations were recorded on a Perkin-Elmer 241 MC polarimeter at 25 °C. $^1$H and $^{13}$C NMR spectra were routinely recorded on a General Electric QE-300 instrument at room temperature. The chemical shifts were referenced to residual protic $C_6D_6$ peaks ($^1$H, $\delta$ = 7.15 ppm; $^{13}$C, $\delta$ = 128.0 ppm). Variable-temperature $^1$H NMR spectra were recorded on a GN-300 NMR spectrometer in toluene-$d_8$ solutions of the respective compounds and were referenced to the residual $CH_3$ peak of toluene ($^1$H, $\delta$ = 2.09 ppm). Elemental analyses were performed by Galbraith Laboratories, Knoxville, TN.

**Preparation of [$Me_2Al(\mu$-*l*-mentholate)]$_2$ (1a).** *l*-Menthol (1 g, 6.40 mmol) was dissolved in pentane (60 mL), and $Me_3Al$ solution (3.20 mL, 6.40 mmol) was added from a syringe as quickly as permitted by the evolution of methane gas (ca. 5 min). The resulting reaction was rapid and exothermic, bringing the pentane to reflux. Tetrahydrofuran (10 mL) was added to this solution, which was then stirred for 2 h. The volume of the solution was slowly reduced in vacuo to leave a white semisolid. The product was purified by dissolving it in 10 mL of pentane, from which it was recrystallized on cooling to −20 °C for a period of 12 h. The white crystalline product was collected, washed with 10–15 mL of very cold pentane, and dried in vacuo. This solid was identified as [$Me_2Al(\mu$-*l*-mentholate)]$_2$: yield 80%; mp 118–120 °C. Anal. Calcd for $C_{12}H_{25}OAl$: C, 67.89; H, 11.87. Found: C, 66.93; H, 11.81. $^1$H NMR ($C_6D_6$): $\delta$ 3.54 (m, 1 H), 2.38 (m, 1 H), 2.10 (m, 1 H), 1.43 (m, 2 H), 1.17 (m overlapping m, 3 H), 0.90 (d, 3 H), 0.80 (d, 3 H), 0.74 (d overlapping m, 5 H), −0.42 (s, 6 H). Partial $^1$H and $^{13}$C NMR spectral results are presented in Tables I and II.

In a separate experiment, 10 mL of THF was added during the final workup, and the solution was stirred for 2 h. The solvent was then removed under vacuum and the product recrystallized from pentane. The $^1$H NMR spectrum of this material was identical with that of **1a**, showing no retention of THF.

**Preparation of [$Et_2Al(\mu$-*l*-mentholate)]$_2$ (1b).** The procedure for this reaction is the same as that for **1a** using *l*-menthol (1.05 g, 6.72 mmol) and $Et_3Al$ solution (3.54 mL, 6.72 mmol). The volume of the solution was slowly reduced in vacuo to leave a viscous oil. This oil was identified as [$Et_2Al(\mu$-*l*-mentholate)]$_2$: yield 85%. $^1$H NMR ($C_6D_6$): $\delta$ 3.57 (m, 1 H), 2.34 (m, 1 H), 2.17 (m, 1 H), 1.32 (t overlapping m, $^3J$ = 9 Hz, 11 H), 0.93 (d, 3 H), 0.83 (d, 3 H), 0.77 (d overlapping m, 5 H), 0.20 (m, 4 H). Partial $^1$H and $^{13}$C NMR spectral results are presented in Tables I and II.

In a separate experiment, 10 mL of $Et_2O$ was added and the product crystallized from the reaction mixture at −20 °C. This was washed with cold pentane. The $^1$H NMR spectrum showed no evidence of ether retention.

**Preparation of [$(i\text{-Bu})_2Al(\mu$-*l*-mentholate)]$_2$ (1c).** The procedure for this reaction is the same as that for **1a** using *l*-menthol (2.19 g, 0.014 mol) and $(i\text{-Bu})_3Al$ solution (14.0 mL, 14 mmol). The volume of the solution was slowly reduced in vacuo to leave a white solid. The product was recrystallized by dissolving it in 10 mL of pentane and cooling at −20 °C for 12 h. The white crystalline solid was collected, washed with 10–15 mL of very cold pentane, and dried in vacuo. This solid was identified as [$(i\text{-Bu})_2Al(\mu$-*l*-mentholate)]$_2$: yield 90%; mp 131–133 °C. $^1$H NMR ($C_6D_6$): $\delta$ 3.62 (m, 1 H), 2.29 (m, 1 H), 2.19 (m, 1 H), 2.05 (m, 2 H), 1.48 (m, 2 H), 1.29 (m, 2 H), 1.13 (d overlapping m, $^3J$ = 6 Hz, 7 H), 1.11 (d, $^3J$ = 6 Hz, 6 H), 0.93 (d, 3 H), 0.84 (d, 3 H), 0.78 (d overlapping m, 5 H), 0.26 (dd, $^2J$ = 14 Hz, $^3J$ = 8 Hz, 2 H), 0.18 (dd, $^2J$ = 14 Hz, $^3J$ = 8 Hz, 2 H). Partial $^1$H and $^{13}$C NMR spectral results are presented in Tables I and II.

**Preparation of [$Me_2Al(\mu$-*l*-borneolate)]$_2$ (2a).** The procedure for this reaction is same as described above using *l*-borneol (1 g, 6.49 mmol) and $Me_3Al$ solution (3.25 mL, 6.49 mmol). The solvent was completely removed in vacuo to leave a white solid. The product was recrystallized by dissolving it in pentane (ca. 10 mL) and cooling to −20 °C. The solid was collected, washed with 10–15 mL of cold pentane, and dried in vacuo. The solid was identified as [$Me_2Al(\mu$-*l*-borneolate)]$_2$: yield 70%; mp 209–211 °C. $^1$H NMR ($C_6D_6$): $\delta$ 4.25 (m, 1 H), 2.20 (m, 1 H), 2.04 (m, 1 H), 1.62 (m, 1 H), 1.45 (t, 1 H), 1.22 (dd overlapping m, 3 H), 0.91 (s, 3 H), 0.68 (s, 3 H), 0.62 (s, 3 H), −0.42 (s, 6 H). Partial $^1$H and

**Table II. $^{13}$C NMR Chemical Shifts ($\delta$ in ppm) in $C_6D_6$**

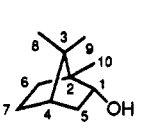


*l*-borneol

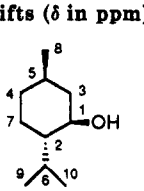


*l*-menthol

| compd | alkyl α-C | alkyl β-C | alkyl γ-C | alkoxide C(1) | C(2) | C(3) | C(4) | C(5) | C(6) | C(7) | C(8) | C(9) | C(10) |
|---|---|---|---|---|---|---|---|---|---|---|---|---|---|
| *l*-menthol | | | | 71.3 | 50.4 | 45.6 | 34.9 | 31.9 | 26.0 | 23.6 | 22.4 | 21.2 | 16.4 |
| *l*-borneol | | | | 76.9 | 49.7 | 48.0 | 45.6 | 39.2 | 28.7 | 26.3 | 20.3 | 18.8 | 13.6 |
| $Me_3Al$ | −7.3 | | | | | | | | | | | | |
| $Et_3Al$ | 0.4 | 8.8 | | | | | | | | | | | |
| $(i\text{-Bu})_3Al$ | 21.4 | 26.3 | 28.3 | | | | | | | | | | |
| **1a** | −8.0 | | | 74.5 | 50.5 | 45.6 | 34.3 | 32.0 | 25.0 | 22.8 | 22.1 | 21.2 | 15.7 |
| **1b** | 1.5 | 9.3 | | 74.8 | 50.5 | 45.7 | 34.3 | 32.1 | 25.1 | 22.9 | 22.2 | 21.2 | 16.0 |
| **1c** | 24.5 | 26.3 | 29.1<br>28.9 | 75.0 | 50.0 | 46.1 | 34.4 | 32.3 | 24.8 | 23.2 | 22.3 | 21.3 | 16.6 |
| **2a** | −8.2 | | | 80.7 | 50.0 | 48.0 | 45.2 | 39.0 | 28.4 | 26.4 | 20.2 | 18.5 | 14.3 |
| **2b** | 1.5 | 9.3 | | 81.0 | 50.1 | 48.1 | 45.1 | 38.9 | 28.6 | 26.4 | 20.2 | 18.5 | 14.3 |
| **2c** | 23.9 | 26.1 | 28.7 | 81.3 | 50.1 | 48.2 | 45.0 | 39.1 | 28.9 | 26.8 | 20.3 | 18.5 | 14.8 |

**Table III. Experimental Parameters for the X-ray Diffraction Study of $[Me_2Al(\mu\text{-}l\text{-mentholate})]_2$ (1a), $[(i\text{-}Bu)_2Al(\mu\text{-}l\text{-mentholate})]_2$ (1c), and $[Me_2Al(\mu\text{-}l\text{-borneolate})]_2$ (2a)**

| | 1a | 1c | 2a |
|---|---|---|---|
| formula | $C_{24}H_{50}Al_2O_2$ | $C_{36}H_{74}Al_2O_2$ | $C_{24}H_{46}Al_2O_2$ |
| mol wt | 424.62 | 592.95 | 420.60 |
| cryst color | colorless | colorless | colorless |
| crystal syst | orthorhombic | triclinic | monoclinic |
| space group | $P2_12_12_1$ (No. 19) | $P\bar{1}$ (No. 1) | $P2_1$ (No. 4) |
| cell constants constrained from 25 high-angle rflns | | | |
| $a$, Å | 10.097 (1) | 10.838 (4) | 7.261 (7) |
| $b$, Å | 10.485 (1) | 12.792 (6) | 14.494 (8) |
| $c$, Å | 26.920 (4) | 15.787 (7) | 12.938 (7) |
| $\alpha$, deg | 90.000 | 81.56 (4) | 90.000 |
| $\beta$, deg | 90.000 | 83.04 (4) | 93.63 (7) |
| $\gamma$, deg | 90.000 | 73.01 (3) | 90.000 |
| $Z$ | 4 | 2 | 2 |
| $V$, Å$^3$ | 2850.3 (7) | 2063.2 (2) | 1358.8 (1.8) |
| density (calc), g cm$^{-3}$ | 0.98 | 0.95 | 1.04 |
| radiation type | Cu K$\bar{\alpha}$ ($\lambda$ = 1.541 78 Å), Ni filtered | Mo K$\bar{\alpha}$ ($\lambda$ = 0.710 73 Å), with a graphite monochromator | Cu K$\bar{\alpha}$ ($\lambda$ = 1.541 78 Å), Ni filtered |
| temp, °C | 0 | 20 | 20 |
| type of data collection | $\theta/2\theta$ scan | $\theta/2\theta$ scan | $\theta/2\theta$ scan |
| $2\theta$ scan range, deg | 8–100 | 6–50 | 8–100 |
| octants used | $+h,+k,+l; -h,-k,-l$ | $+h,\pm k,\pm l$ | $+h,\pm k,\pm l$ |
| scan rate, deg min$^{-1}$ | variable, 3–8 | variable 4–29 | variable 3–8 |
| scan range | 1.0–1.2 | 1–1.1 | 1.2–1.3 |
| std rflns | 3 measd per every 100 rflns; no significant deviation from the standard obsd | | |
| no. of data collected: | 5744 | 7289 | 1622 |
| no. of unique rflns | 3592 | 7288 | 1442 |
| no. of obsd rflns | 2669 ($F_o \geq 2.5\sigma(F)$) | 4213 ($F_o \geq 3.0\sigma(F)$) | 1432 ($F_o \geq 2.5\sigma(F)$) |
| linear abs coeff ($\mu$), cm$^{-1}$ | 4.06 | 0.71 | 4.25 |
| $F$(000), e | 944 | 664 | 464 |
| abs cor | none applied | none applied | none applied |
| no. of params refined | 287 | 649 (360 block 1, 289 block 2) | 270 |
| observn/param ratio | 9.3:1 | 5.0:1 | 5.3:1 |
| $R = \sum(\lvert F_o - \lvert F_c\rvert)/\sum\lvert F_o\rvert$, % | 4.5 | 8.7 | 5.3 |
| $R_w = [\sum(\lvert F_o - \lvert F_c\rvert)^2/\sum w\lvert F_o\rvert^2]^{1/2}$, % | 3.9 | 8.5 | 4.4 |
| overall shift/esd | 0.000 | 0.011 | 0.000 |
| max shift/esd | 0.001 | 0.255 | 0.002 |
| residual electron density, eÅ$^{-3}$ | 0.24, 1.69 Å from Al1 | 0.36, 1.54 Å, from C21A | 0.17, 1.58 Å from O2 |

$^{13}$C NMR spectral results are presented in Tables I and II.

**Preparation of $[Et_2Al(\mu\text{-}l\text{-borneolate})]_2$ (2b).** The procedure for this reaction is same as described above using $l$-borneol (1.86 g, 12.1 mmol) and $Et_3Al$ solution (6.35 mL, 12.1 mmol). The solvent was completely removed in vacuo to leave a white solid. The product was recrystallized by dissolving it in pentane (ca. 10 mL) and cooling to −20 °C. The solid was collected, washed with 10–15 mL of cold pentane, and dried in vacuo. The solid was identified as $[Et_2Al(\mu\text{-}l\text{-borneolate})]_2$: yield 88%; mp 216–217 °C. Anal. Calcd for $C_{14}H_{27}AlO$: C, 70.55; H, 11.42. Found: C, 67.39; H, 11.03. $^1$H NMR ($C_6D_6$): $\delta$ 4.36 (m, 1 H), 2.28 (m, 1 H), 2.08 (m, 1 H), 1.65 (m, 1 H), 1.48 (t, 1 H), 1.28 (t overlapping m, $^3J$ = 9 Hz, 9 H), 0.94 (s, 3 H), 0.70 (s, 3 H), 0.67 (s, 3 H), 0.23 (q, $^3J$ = 9 Hz, 4 H). Partial $^1$H and $^{13}$C NMR spectral results are presented in Tables I and II.

**Preparation of $[(i\text{-}Bu)_2Al(\mu\text{-}l\text{-borneolate})]_2$ (2c).** The procedure for this reaction is same as described above using $l$-borneol (1.99 g, 12.9 mmol) and $Al(i\text{-}Bu)_3$ solution (12.9 mL, 12.9 mmol). The solvent was completely removed in vacuo to leave a white solid. The product was recrystallized by dissolving it in pentane (ca. 10 mL) and cooling to −20 °C. The solid was collected, washed with 10–15 mL of cold pentane, and dried in vacuo. The solid was identified as $[(i\text{-}Bu)_2Al(\mu\text{-}l\text{-borneolate})]_2$: yield 89%; mp 124–125 °C. $^1$H NMR ($C_6D_6$): $\delta$ 4.46 (m, 1 H), 2.34 (m, 1 H), 2.04 (m overlapping m, 3 H), 1.66 (m, 1 H), 1.52 (t, 1 H), 1.13 (d overlapping m, $^3J$ = 6 Hz, 15 H), 0.99 (s, 3 H), 0.70 (s, 6 H), 0.28 (d, $^3J$ = 6 Hz, 4 H). Partial $^1$H and $^{13}$C NMR spectral results are presented in Tables I and II.

**Structure Determination and Refinement of $[Me_2Al(\mu\text{-}l\text{-mentholate})]_2$ (1a), $[(i\text{-}Bu)_2Al(\mu\text{-}l\text{-mentholate})]_2$ (1c), and $[Me_2Al(\mu\text{-}l\text{-borneolate})]_2$ (2a).** Crystals of **1a** and **2a** were grown slowly from a pentane solution at −20 °C; X-ray-quality crystals of **1c** were more difficult to obtain and formed at the interface between the solution and gas phase after several months in the freezer. In each case, a crystal suitable for X-ray diffraction was mounted in a thin-walled capillary tube in the drybox and the tube was plugged with grease, removed from the drybox, flame-sealed, mounted on a goniometer head, and placed on a P3/V diffractometer for data collection. The crystal and X-ray data collection parameters for **1a**,**c** and **2a** are listed in Table III.

Compound **1a** was found to be orthorhombic and was assigned to the space group $P2_12_12_1$ (No. 19) on the basis of the systematic absence $0k0$ ($k = 2n + 1$). An initial data set for **1c** was collected using Cu radiation and was solved in the triclinic cell system, space group $P\bar{1}$ (No. 1). The structure could not be refined well because of high thermal motion/disorder and was further limited because of the small number of observed data. A second data set was collected on the best available crystal with Mo radiation. The new data set gave almost identical results, even though a few additional observed data were obtained. Compound **2a** was found to be monoclinic and was assigned to the space group $P2_1$ (No. 4) on the basis of the systematic absence $0k0$ ($k = 2n + 1$). Unit cell parameters were derived from the least-squares fit of the angular settings of 25 reflections with $40° < 2\theta < 80°$ for **1a** and **2a** and of 25 reflections with $20° < 2\theta < 30°$ for **1c**. Data reduction and calculations were carried out using the SHELXTL programs.[9] The structure of **1a** was solved by the Patterson heavy-atom method, while the structures of both **1c** and **2a** were solved by direct methods. Refinement was carried out using the SHELX-76 set of programs.[10]

Full-matrix least-squares refinement of positional and thermal parameters for non-hydrogen atoms was carried out by the minimizing function $\sum(w\lvert F_o\rvert - \lvert F_c\rvert)^2$, where $\lvert F_o\rvert$ and $\lvert F_c\rvert$ are the observed and calculated structural factors, respectively. The weighting scheme used on the last cycle was $w = 1.5531/\sigma^2(F_o)$

(9) Sheldrick, G. M. SHELXTL; University of Gottingen: Gottingen, Federal Republic of Germany, 1978.
(10) Sheldrick, G. M. SHELX-76; University Chemical Laboratory: Cambridge, England, 1976.

**Table IV. Atomic Coordinates and Isotropic Thermal Parameters for the Non-Hydrogen Atoms of $[Me_2Al(\mu\text{-}l\text{-mentholate})]_2$ (1a)**

| atom | x | y | z | $U_{eq}$,[a] Å$^2$ |
|---|---|---|---|---|
| Al1 | 0.2525 (1) | 0.0802 (1) | 0.15796 (4) | 0.0503 (4) |
| Al2 | 0.0828 (1) | −0.0445 (1) | 0.09116 (5) | 0.0525 (5) |
| O1 | 0.2595 (3) | −0.0363 (2) | 0.10680 (8) | 0.0496 (9) |
| O2 | 0.0750 (3) | 0.0693 (2) | 0.14343 (8) | 0.0477 (9) |
| C1 | 0.3191 (5) | 0.2511 (4) | 0.1418 (2) | 0.079 (2) |
| C2 | 0.2960 (5) | 0.0031 (4) | 0.2226 (1) | 0.085 (2) |
| C3 | 0.0497 (5) | 0.0292 (5) | 0.0252 (1) | 0.081 (2) |
| C4 | 0.0051 (4) | −0.2112 (4) | 0.1060 (2) | 0.081 (2) |
| C5 | 0.3673 (4) | −0.0874 (4) | 0.0775 (2) | 0.051 (2) |
| C6 | 0.4415 (4) | 0.0212 (4) | 0.0525 (2) | 0.055 (2) |
| C7 | 0.5572 (5) | −0.0237 (4) | 0.0203 (2) | 0.061 (2) |
| C8 | 0.6474 (4) | −0.1078 (4) | 0.0517 (2) | 0.068 (2) |
| C9 | 0.5735 (5) | −0.2169 (4) | 0.0762 (2) | 0.067 (2) |
| C10 | 0.4578 (4) | −0.1718 (4) | 0.1085 (2) | 0.051 (2) |
| C11 | 0.3842 (5) | −0.2818 (4) | 0.1348 (2) | 0.062 (2) |
| C12 | 0.4706 (5) | −0.3400 (4) | 0.1767 (2) | 0.088 (2) |
| C13 | 0.3356 (5) | −0.3864 (4) | 0.1000 (2) | 0.088 (2) |
| C14 | 0.6306 (5) | 0.0901 (4) | −0.0026 (2) | 0.082 (2) |
| C15 | −0.0271 (4) | 0.1540 (4) | 0.1622 (2) | 0.048 (2) |
| C16 | −0.0582 (4) | 0.2540 (4) | 0.1231 (1) | 0.056 (2) |
| C17 | −0.1670 (5) | 0.3455 (4) | 0.1389 (2) | 0.068 (2) |
| C18 | −0.2901 (4) | 0.2698 (4) | 0.1525 (2) | 0.072 (2) |
| C19 | −0.2599 (5) | 0.1689 (4) | 0.1923 (2) | 0.072 (2 |
| C20 | −0.1475 (4) | 0.0781 (4) | 0.1775 (2) | 0.055 (2) |
| C21 | −0.1194 (5) | −0.0247 (5) | 0.2175 (2) | 0.073 (2) |
| C22 | −0.0899 (5) | 0.0312 (5) | 0.2693 (2) | 0.094 (2) |
| C23 | −0.2309 (6) | −0.1232 (5) | 0.2201 (2) | 0.110 (3) |
| C24 | −0.1966 (5) | 0.4443 (4) | 0.0987 (2) | 0.104 (2) |

[a] $U_{eq} = {}^1/_3\sum_i\sum_j U_{ij}(a_i^*\cdot a_j^*)(\bar{a}_i\cdot\bar{a}_j)$.

**Scheme I**

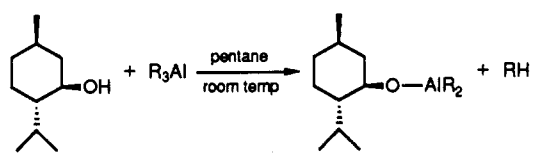


**1a**, R = Me (80%)
**b**, R = Et (85%)
**c**, R = *i*-Bu (90%)

+ $0.0001(F_o)^2$ for **1a**, $w = 4.4508/\sigma^2(F_o) + 0.00005(F_o)^2$ for **1c**, and $w = 1.3360/\sigma^2(F_o) + 0.00001(F_o)^2$ for **2a**. The scattering factors for neutral carbon, oxygen, and aluminum were used.[11] The data were corrected for Lorentz and polarization effects in all cases. Absorption corrections were not necessary because of very low linear absorption coefficients. The hydrogen atoms were placed in calculated positions riding on the respective carbon atoms. Their isotropic thermal parameters were refined as free variables during the refinement.

The structures of **1a** and **2a** were refined satisfactorily. In **1c**, several problems were encountered. First, the crystal quality was poor, and all attempts to obtain better crystals were unsuccessful. Second, there was a disorder problem associated with the isobutyl groups attached to aluminum which could not be modeled effectively; therefore, the C–C distances C33A–C34A, C34A–C35A, and C34A–C36A in this group were fixed at 1.50 Å during refinement. These problems make the distances and angles associated with the isobutyl groups unreliable but do not affect the major structural features that are important to the intramolecular interactions that govern the rotational barrier. In each case, after several cycles of refinement, convergence was achieved with $R = 4.5\%$ and $R_w = 3.9\%$ for **1a**, $R = 8.7\%$ and $R_w = 8.5\%$ for **1c**, and $R = 5.3\%$ and $R_w = 4.4\%$ for **2a**. Additional details concerning data collection and the structure solutions are presented in Table III. Atomic coordinates and isotropic thermal parameters for the non-hydrogen atoms are listed in Tables IV–VI for **1a,c** and **2a**, respectively.

(11) *International Tables for X-ray Crystallography*; Kynoch: Birmingham, England, 1974; Vol. IV (present distributor D. Reidel, Dordrecht, The Netherlands).

**Scheme II**

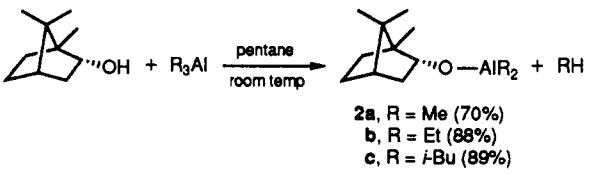


**2a**, R = Me (70%)
**b**, R = Et (88%)
**c**, R = *i*-Bu (89%)

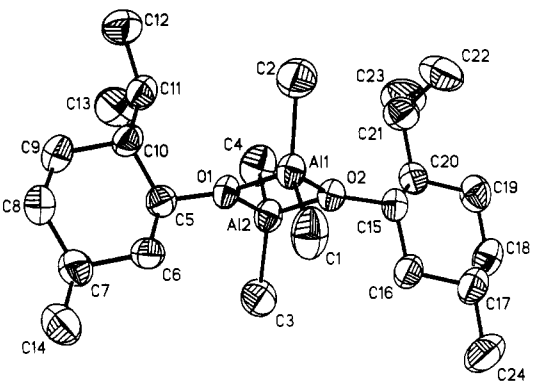


**Figure 1.** ORTEP diagram of the $[Me_2Al(\mu\text{-}l\text{-mentholate})]_2$ dimer (**1a**) with the atoms represented by 50% thermal ellipsoids. Hydrogen atoms have been omitted for clarity.

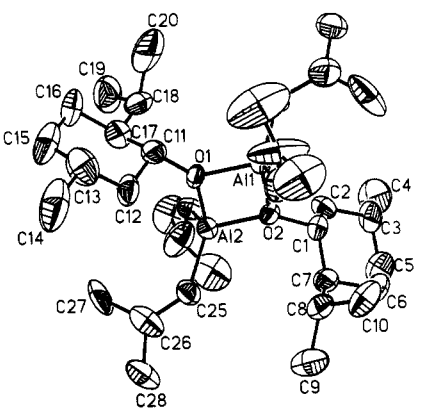


**Figure 2.** ORTEP diagram of the $[(i\text{-Bu})_2Al(\mu\text{-}l\text{-mentholate})]_2$ dimer (**1c**) with the atoms represented by 50% thermal ellipsoids. Hydrogen atoms have been omitted for clarity.

## Results and Discussion

**Synthesis of Optically Active Organoaluminum Alkoxides.** The optically active organoaluminum alkoxides $R_2AlOR'$ (R = Me, Et, *i*-Bu; OR′ = *l*-mentholate, *l*-borneolate) were prepared from the reaction of the optically active alcohol (*l*-menthol or *l*-borneol) with the trialkylaluminum species $R_3Al$ (R = Me, Et, *i*-Bu) in a 1:1 stoichiometry (Schemes I and II) to afford the alkoxide complexes **1a–c** and **2a–c**, and the corresponding alkane RH in high yields of isolated products. The metal derivatives retain their optical activity. The optical rotations show a general trend, decreasing in magnitude as the alkyl substituent increases in bulk (Table VII). Compounds **1a,c** and **2a–2c** have been isolated as colorless, transparent crystals, while **1b** was isolated as a spectroscopically pure semisolid. The complexes are both air- and moisture-sensitive, decomposing over a period of seconds in the solid state after exposure to air. They are very soluble in both hydrocarbons (i.e., pentane, benzene, and toluene) and in donor solvents (i.e., tetrahydrofuran and diethyl ether).

Table V. Atomic Coordinates and Isotropic Thermal Parameters for the Non-Hydrogen Atoms of $[(i\text{-Bu})_2Al(\mu\text{-}l\text{-mentholate})]_2$ (1c)

| atom | x | y | z | $U_{eq}$,[a] Å$^2$ | atom | x | y | z | $U_{eq}$,[a] Å$^2$ |
|---|---|---|---|---|---|---|---|---|---|
| | | | | Molecule 1 | | | | | |
| Al1 | 0.96330 | 0.87600 | 0.16910 | 0.056 (1) | C17 | 0.848 (1) | 0.750 (1) | −0.0162 (8) | 0.084 (6) |
| Al2 | 1.1479 (3) | 0.7857 (2) | 0.0387 (2) | 0.055 (1) | C18 | 0.805 (1) | 0.865 (1) | −0.0565 (9) | 0.095 (7) |
| O1 | 0.9816 (6) | 0.7902 (5) | 0.0815 (4) | 0.053 (3) | C19 | 0.791 (2) | 0.880 (1) | 0.1540 (9) | 0.15 (1) |
| O2 | 1.1297 (6) | 0.8715 (5) | 0.1267 (4) | 0.055 (3) | C20 | 0.665 (2) | 0.926 (1) | −0.0220 (9) | 0.15 (1) |
| C1 | 1.197 (1) | 0.9401 (9) | 0.1556 (7) | 0.059 (5) | C21 | 1.145 (1) | 0.8601 (9) | −0.0747 (7) | 0.077 (5) |
| C2 | 1.193 (1) | 1.0381 (8) | 0.0896 (8) | 0.073 (5) | C22 | 1.257 (2) | 0.848 (2) | −0.142 (1) | 0.16 (1) |
| C3 | 1.258 (2) | 1.117 (1) | 0.120 (1) | 0.101 (7) | C23 | 1.226 (2) | 0.911 (1) | −0.2258 (9) | 0.138 (9) |
| C4 | 1.250 (2) | 1.216 (1) | 0.054 (1) | 0.20 (1) | C24 | 1.368 (2) | 0.864 (1) | −0.112 (1) | 0.15 (1) |
| C5 | 1.394 (2) | 1.057 (1) | 0.138 (1) | 0.14 (1) | C25 | 1.275 (1) | 0.6443 (8) | 0.0678 (7) | 0.076 (5) |
| C6 | 1.399 (1) | 0.961 (1) | 0.201 (1) | 0.15 (1) | C26 | 1.340 (2) | 0.561 (1) | 0.012 (1) | 0.130 (9) |
| C7 | 1.331 (1) | 0.8787 (9) | 0.1764 (9) | 0.080 (6) | C27 | 1.267 (2) | 0.534 (1) | −0.049 (1) | 0.17 (1) |
| C8 | 1.345 (1) | 0.777 (1) | 0.2427 (9) | 0.088 (7) | C28 | 1.442 (2) | 0.460 (1) | 0.052 (1) | 0.15 (1) |
| C9 | 1.304 (1) | 0.802 (1) | 0.3340 (9) | 0.124 (8) | C29 | 0.970 (1) | 0.788 (1) | 0.2857 (8) | 0.096 (7) |
| C10 | 1.472 (1) | 0.697 (1) | 0.233 (1) | 0.149 (9) | C30 | 0.862 (1) | 0.782 (1) | 0.345 (1) | 0.18 (1) |
| C11 | 0.885 (1) | 0.735 (1) | 0.0736 (7) | 0.075 (6) | C31 | 0.890 (2) | 0.704 (2) | 0.421 (1) | 0.21 (1) |
| C12 | 0.936 (1) | 0.612 (1) | 0.1087 (9) | 0.094 (7) | C32 | 0.743 (2) | 0.805 (2) | 0.329 (1) | 0.23 (2) |
| C13 | 0.842 (2) | 0.550 (1) | 0.106 (1) | 0.117 (9) | C33 | 0.836 (1) | 1.0164 (9) | 0.1419 (8) | 0.078 (6) |
| C14 | 0.892 (2) | 0.433 (1) | 0.136 (1) | 0.16 (1) | C34 | 0.788 (2) | 1.102 (1) | 0.202 (1) | 0.14 (1) |
| C15 | 0.798 (2) | 0.567 (1) | 0.015 (1) | 0.15 (1) | C35 | 0.688 (1) | 1.202 (1) | 0.170 (1) | 0.129 (8) |
| C16 | 0.745 (1) | 0.684 (1) | −0.0158 (9) | 0.105 (7) | C36 | 0.864 (2) | 1.120 (1) | 0.255 (1) | 0.18 (1) |
| | | | | Molecule 2 | | | | | |
| Al3 | 0.9606 (3) | 0.2697 (3) | 0.5555 (2) | 0.061 (1) | C19A | 0.811 (2) | 0.190 (1) | 0.841 (1) | 0.15 (1) |
| Al4 | 1.1347 (3) | 0.3520 (3) | 0.6294 (2) | 0.063 (1) | C20A | 0.949 (2) | 0.245 (1) | 0.912 (1) | 0.16 (1) |
| O3 | 0.9648 (6) | 0.3453 (5) | 0.6442 (4) | 0.062 (3) | C21A | 0.870 (1) | 0.3600 (9) | 0.4593 (7) | 0.081 (3) |
| O4 | 1.1279 (6) | 0.2772 (5) | 0.5389 (4) | 0.061 (3) | C22A | 0.721 (3) | 0.388 (2) | 0.254 (2) | 0.25 (1) |
| C1A | 1.222 (1) | 0.2120 (9) | 0.4791 (7) | 0.064 (5) | C23A | 0.653 (2) | 0.336 (2) | 0.297 (1) | 0.202 (8) |
| C2A | 1.301 (1) | 0.1092 (9) | 0.5279 (8) | 0.083 (6) | C24A | 0.696 (2) | 0.422 (2) | 0.368 (1) | 0.28 (1) |
| C3A | 1.407 (2) | 0.036 (1) | 0.475 (1) | 0.122 (8) | C25A | 0.930 (1) | 0.1286 (9) | 0.6005 (7) | 0.089 (4) |
| C4A | 1.483 (1) | −0.061 (1) | 0.524 (1) | 0.155 (9) | C26A | 0.902 (1) | 0.057 (1) | 0.5414 (9) | 0.105 (4) |
| C5A | 1.488 (1) | 0.104 (1) | 0.422 (1) | 0.132 (9) | C27A | 1.011 (2) | 0.013 (1) | 0.485 (1) | 0.167 (6) |
| C6A | 1.409 (1) | 0.204 (1) | 0.3701 (9) | 0.113 (7) | C28A | 0.854 (2) | −0.034 (1) | 0.594 (1) | 0.170 (7) |
| C7A | 1.304 (1) | 0.278 (1) | 0.4271 (8) | 0.079 (5) | C29A | 1.153 (1) | 0.4965 (9) | 0.5851 (7) | 0.089 (4) |
| C8A | 1.222 (1) | 0.382 (1) | 0.3753 (9) | 0.107 (8) | C30A | 1.185 (2) | 0.573 (2 | 0.641 (1) | 0.175 (7) |
| C9A | 1.303 (1) | 0.465 (1) | 0.346 (1) | 0.146 (9) | C31A | 1.226 (2) | 0.664 (2) | 0.592 (1) | 0.27 (1) |
| C10A | 1.171 (2) | 0.357 (1) | 0.2959 (8) | 0.16 (1) | C32A | 1.110 (2) | 0.597 (1) | 0.712 (1) | 0.206 (8) |
| C11A | 0.843 (1) | 0.393 (1) | 0.6947 (9) | 0.100 (7) | C33A | 1.235 (1) | 0.2589 (9) | 0.7223 (7) | 0.079 (3) |
| C12A | 0.787 (1) | 0.516 (1) | 0.6607 (8) | 0.096 (7) | C34A | 1.383 (1) | 0.233 (1) | 0.716 (1) | 0.100 (3) |
| C13A | 0.679 (2) | 0.569 (1) | 0.704 (2) | 0.18 (1) | C34B | 1.362 (1) | 0.267 (2) | 0.752 (1) | 0.100 (3) |
| C14A | 0.629 (2) | 0.684 (2) | 0.670 (1) | 0.31 (2) | C35B | 1.424 (2) | 0.180 (2) | 0.824 (1) | 0.100 (3) |
| C15A | 0.678 (2) | 0.537 (2) | 0.801 (1) | 0.20 (2) | C35A | 1.453 (2) | 0.122 (2) | 0.765 (2) | 0.100 (3) |
| C16A | 0.719 (2) | 0.427 (2) | 0.835 (1) | 0.15 (1) | C36A | 1.405 (2) | 0.326 (2) | 0.760 (1) | 0.100 (3) |
| C17A | 0.857 (1) | 0.373 (1) | 0.7878 (9) | 0.096 (7) | C36B | 1.461 (2) | 0.252 (2) | 0.673 (1) | 0.100 (3) |
| C18A | 0.901 (1) | 0.261 (1) | 0.8271 (9) | 0.095 (7) | | | | | |

[a] See footnote a of Table IV.

The ether solvents do not appear to form a stable isolable addition complex.

**X-ray Structures.** The structures of the two menthol derivatives $[Me_2Al(\mu\text{-}l\text{-mentholate})]_2$ (**1a**) and $[(i\text{-Bu})_2Al(\mu\text{-}l\text{-mentholate})]_2$ (**1c**) and of the borneol derivative $[Me_2Al(\mu\text{-}l\text{-borneolate})]_2$ (**2a**) have been determined by single-crystal X-ray diffraction methods. All three compounds have the same general structural features with the formation of oxygen-bridged dimers. The ORTEP diagrams are shown in Figures 1–3 for **1a,c** and **2a**, respectively. They show similar features for all three compounds with virtually planar central four-membered $Al_2O_2$ rings with the alkyl groups bound to the aluminum atoms in a plane perpendicular to the $Al_2O_2$ plane. The Al–O bond distances range from 1.839 to 1.842 Å, somewhat less than the Al–O distance found in $[Me_2Al(\mu\text{-}2\text{-allyl-}6\text{-methylphenoxide})]_2$[12] or in the dinuclear five-coordinate organoaluminum complexes $[Me_2Al\{\mu\text{-}O(CH_2)_2OMe\}]_2$[13] and $[Me_2Al\{\mu\text{-}OCH_2\text{-}2\text{-}(C_5H_4N)\}]_2$[14] or in $[Me_2Al(\mu\text{-}O\text{-}t\text{-Bu})]_2$ (gas).[16] The observed distances in these compounds are, however, significantly longer than the Al–O bond distance in the mononuclear tetrahedral organoaluminum alkoxides $Me_2AlBHT\cdot PMe_3$[17] and $Et_2AlBHT\cdot CH_3C_6H_4CO_2Me$.[18]

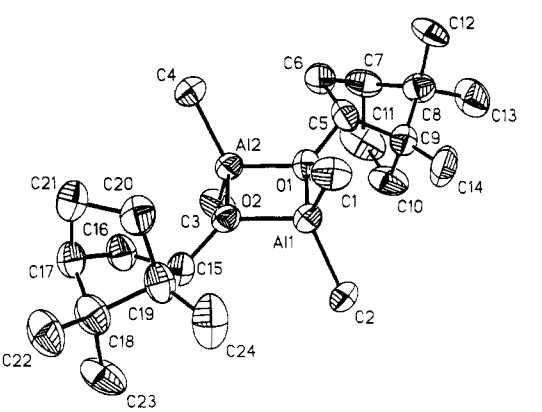


**Figure 3.** ORTEP diagram of the $[Me_2Al(\mu\text{-}l\text{-borneolate})]_2$ dimer (**2a**) with the atoms represented by 50% thermal ellipsoids. Hydrogen atoms have been omitted for clarity.

(12) Kumar, R.; Sierra, M. L.; de Mel, V. S. J.; Oliver, J. P. *Organometallics* **1990**, *9*, 484.
(13) Benn, R.; Rufińska, A.; Lehmkuhl, H.; Janssen, E.; Krüger, C. *Angew. Chem., Int. Ed. Engl.* **1983**, *22*, 779.
(14) van Vliet, M. R. P.; Buysingh, P.; van Koten, G.; Vrieze, K.; Kojić-Prodić, B.; Spek, A. L. *Organometallics* **1985**, *4*, 1701.
(15) Uhl, W. *Z. Naturforsch.* **1988**, *43B*, 1113.
(16) Haaland, A.; Stokkeland, O. *J. Organomet. Chem.* **1975**, *94*, 345.

**Table VI. Atomic Coordinates and Isotropic Thermal Parameters for the Non-Hydrogen Atoms of $[Me_2Al(\mu\text{-}l\text{-borneolate})]_2$ (2a)**

| atom | x | y | z | $U_{eq}$,[a] Å$^2$ |
|---|---|---|---|---|
| Al1 | 0.2854 (3) | 0.32130 | 0.6575 (2) | 0.0703 (8) |
| Al2 | 0.1724 (3) | 0.3597 (2) | 0.8542 (2) | 0.0717 (8) |
| O1 | 0.2792 (6) | 0.4184 (4) | 0.7481 (3) | 0.069 (2) |
| O2 | 0.1765 (6) | 0.2607 (3) | 0.7628 (3) | 0.068 (2) |
| C1 | 0.5404 (9) | 0.2840 (5) | 0.6452 (6) | 0.096 (3) |
| C2 | 0.1091 (9) | 0.3282 (6) | 0.5372 (5) | 0.097 (3) |
| C3 | −0.079 (1) | 0.4063 (6) | 0.8651 (6) | 0.099 (4) |
| C4 | 0.344 (1) | 0.3398 (6) | 0.9756 (5) | 0.111 (4) |
| C5 | 0.399 (1) | 0.4995 (7) | 0.7585 (6) | 0.089 (4) |
| C6 | 0.372 (1) | 0.5602 (6) | 0.8607 (6) | 0.105 (4) |
| C7 | 0.336 (1) | 0.6551 (7) | 0.8171 (9) | 0.100 (4) |
| C8 | 0.450 (1) | 0.6587 (7) | 0.7240 (7) | 0.090 (4) |
| C9 | 0.362 (1) | 0.5722 (6) | 0.6732 (6) | 0.087 (3) |
| C10 | 0.158 (1) | 0.5981 (7) | 0.6701 (8) | 0.122 (5) |
| C11 | 0.140 (1) | 0.6537 (7) | 0.773 (1) | 0.142 (5) |
| C12 | 0.657 (1) | 0.6507 (8) | 0.7528 (8) | 0.145 (5) |
| C13 | 0.428 (1) | 0.7489 (6) | 0.6622 (8) | 0.136 (5) |
| C14 | 0.431 (1) | 0.5440 (7) | 0.5713 (6) | 0.133 (5) |
| C15 | 0.045 (1) | 0.1825 (5) | 0.7600 (6) | 0.079 (3) |
| C16 | −0.041 (1) | 0.1644 (6) | 0.8669 (6) | 0.108 (4) |
| C17 | 0.008 (1) | 0.0630 (6) | 0.8899 (7) | 0.098 (4) |
| C18 | 0.001 (1) | 0.0187 (6) | 0.7806 (8) | 0.103 (4) |
| C19 | 0.140 (1) | 0.0901 (5) | 0.7357 (6) | 0.086 (3) |
| C20 | 0.306 (1) | 0.0819 (7) | 0.8139 (8) | 0.111 (4) |
| C21 | 0.220 (1) | 0.0584 (7) | 0.9178 (8) | 0.144 (5) |
| C22 | 0.056 (1) | −0.0825 (6) | 0.7772 (8) | 0.137 (5) |
| C23 | −0.197 (1) | 0.0206 (6) | 0.7269 (7) | 0.119 (4) |
| C24 | 0.178 (1) | 0.0769 (7) | 0.6257 (7) | 0.141 (5) |

[a] See footnote *a* of Table IV.

**Table VII. Optical Rotations of the Optically Active Alkylaluminum Alkoxides at 25 °C**

| compd | $[\alpha]^{25}$, deg | concn, *c* | compd | $[\alpha]^{25}$, deg | concn, *c* |
|---|---|---|---|---|---|
| *l*-menthol | −46.1 | 1.01 | *l*-borneol | −35.2 | 1.05 |
| **1a** | −46.2 | 0.69 | **2a** | −17.9 | 0.71 |
| **1b** | −24.2 | 0.91 | **2b** | −14.0 | 1.26 |
| **1c** | −30.7 | 1.41 | **2c** | −9.8 | 1.17 |

[a] Concentration is in g/100 mL of solvent (toluene).

The Al–C bond lengths range from 1.942 to 1.963 Å in **1a,c** and **2a** and are in the typical range for Al–C bond distances (see Table IX).

The coordination geometry around the aluminum atom is distorted from tetrahedral symmetry in each case. The internal Al–O–Al and O–Al–O angles for these compounds, along with a number of other oxygen-bridged molecules, are summarized in Table IX. The internal O–Al–O angles (*a*; see structure I) and Al–O–Al (*b*, I) are 80 ± 2 and 100 ± 2°, respectively. The external C–Al–C angles (*c*; I) range from 118.7 to 122.3° and are consistent with the observed C–Al–C angles in other oxygen-bridged dimers. Finally, it should be noted that the external O–Al–C angles (*d*; I) range from 108 to 115°. The other structural parameter sometimes used to characterize these ring systems is the Al···Al separation. In these molecules this distance ranges

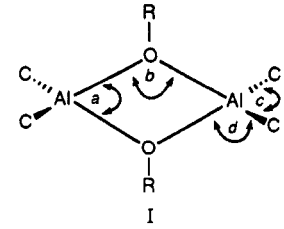


I

from 2.779 to 2.840 Å and is dependent on the other parameters that define the ring, the Al–O distances, and the internal angles already discussed. This metal–metal separation is somewhat less than that observed in other alkoxide-bridged compounds such as $[Me_2Al(\mu\text{-}2\text{-allyl-}6\text{-methylphenoxide})]_2$[12] with an Al···Al separation of 2.866 Å. Much longer Al···Al contact distances of 2.924 and 3.02 Å have been found in the five-coordinate aluminum derivatives $[Me_2Al\{\mu\text{-}O(CH_2)_2OCH_3\}]_2$[13] and $[Me_2Al\{\mu\text{-}OCH_2\text{-}2\text{-}(C_5H_4N)\}]_2$.[14] However, the distances observed in these compounds are significantly longer than the single Al–Al bond distance of 2.66 Å recently reported in $[(Me_3Si)_2CH]_2Al\text{–}Al[CH(SiMe_3)_2]_2$[15] and are consistent with the Al···Al distances observed in other oxygen- and nitrogen-bridged organoaluminum derivatives.

Examination of the three structures provides some additional insight into the behavior of these molecules, both in the solid state and in solution. As the bulk of the substituents on the metal increases between **1a** and **1c**, the alkyl group bound to the aluminum interacts more strongly with the substituent in the 2-position on the menthol moiety and causes these two derivatives to assume different conformations in the solid state. In the methyl mentholate derivative **1a**, there appears to be only a modest interaction between the isopropyl group in the 2-position on the menthol ring and the methyl groups bound to the aluminum. The menthol groups are in the syn conformation in the solid state and are tilted slightly to minimize the intramolecular interactions. This conformation is likely the result of packing forces. In the isobutyl derivative, both the menthol groups and the isobutyl groups are oriented in the anti conformation, which results from intramolecular interactions. In the borneol derivative **2a**, there is no steric interaction, and the molecule adopts the configuration of lowest energy and most efficient packing.

**NMR Studies.** The major features of the $^1H$ and $^{13}C$ NMR spectra of the compounds **1a–c** and **2a–c** are listed in Tables I and II. They are generally consistent with the reactions and structures described. There is no evidence of the –OH groups of the starting alcohols, and the *l*-mentholate or *l*-borneolate groups show modest changes in chemical shift consistent with alkoxide bridge formation. The $^{13}C$ NMR spectra of the compounds **1a–c** and **2a–c** show that the resonance due to C(1) is shifted downfield while the resonances due to C(2)–C(10) are relatively unaffected upon complex formation. These shift effects can be attributed to the overall electron-withdrawing ability of the $-OAlR_2$ moiety. The $^{13}C$ chemical shifts of the alkyl groups bound to the aluminum upon complexation were also shifted slightly from the corresponding resonance in the parent $R_3Al$. The observation that the γ-carbon atoms of the isobutyl group in **1c** are nonequivalent, showing two lines at 28.9 and 29.1 ppm, is of particular interest since this indicates that there is hindered rotation in the molecule.

Examination of the $^1H$ NMR spectra of the alkyl groups of the dialkylaluminum moiety in the *l*-mentholate derivatives reveals some interesting features. The $^1H$ NMR spectrum of $[Me_2Al(\mu\text{-}l\text{-mentholate})]_2$ shows no unusual

(17) Healy, M. D.; Wierda, D. A.; Barron, A. R. *Organometallics* **1988**, *7*, 2543.
(18) Shreve, A. P.; Mulhaupt, R.; Fultz, W.; Calabrese, J.; Robbins, W.; Ittel, S. D. *Organometallics* **1988**, *7*, 409.
(19) Haaland, A.; Samdal, S.; Stokkeland, O.; Weidlein, J. *J. Organomet. Chem.* **1977**, *134*, 165.
(20) Zaworotko, M. J.; Kerr, C. R.; Atwood, J. L. *Organometallics* **1985**, *4*, 238.
(21) Atwood, J. L.; Zaworotko, M. J. *J. Chem. Soc., Chem. Commun.* **1983**, 302.
(22) Garbauskas, M. F.; Wengrovius, J. H.; Going, R. C.; Kasper, J. S. *Acta Crystallogr., Sect. C* **1984**, *C40*, 1536.
(23) Kai, Y.; Yasuoka, N.; Kasai, N.; Kakudo, M. *Bull. Chem. Soc. Jpn.* **1972**, *45*, 3397.
(24) Sierra, M. L.; de Mel, V. S. J.; Oliver, J. P. *Organometallics* **1989**, *8*, 2486.

**Table VIII. Selected Bond Lengths (Å) and Angles (deg) for $[Me_2Al(\mu\text{-}l\text{-mentholate})]_2$ (1a), $[(i\text{-}Bu)_2Al(\mu\text{-}l\text{-mentholate})]_2$ (1c), and $[Me_2Al(\mu\text{-}l\text{-borneolate})]_2$ (2a)**

| 1a | | 1c molecule 1 | | 1c molecule 2 | | 2a | |
|---|---|---|---|---|---|---|---|
| | | | Bond Lengths | | | | |
| Al1–Al2 | 2.807 (2) | Al1–Al2 | 2.815 (3) | Al3–Al4 | 2.843 (6) | Al1–Al2 | 2.779 (3) |
| Al1–O1 | 1.843 (2) | Al1–O1 | 1.847 (8) | Al3–O3 | 1.83 (1) | Al1–O1 | 1.834 (5) |
| Al1–O2 | 1.838 (3) | Al1–O2 | 1.833 (6) | Al3–O4 | 1.828 (7) | Al1–O2 | 1.840 (5) |
| Al1–C1 | 1.962 (4) | Al1–C29 | 2.01 (2) | Al3–C21A | 1.95 (1) | Al1–C1 | 1.945 (7) |
| Al1–C2 | 1.968 (4) | Al1–C33 | 1.94 (1) | Al3–C25A | 1.94 (2) | Al1–C2 | 1.954 (7) |
| Al2–O1 | 1.835 (3) | Al2–O1 | 1.834 (7) | Al4–O3 | 1.854 (8) | Al2–O1 | 1.829 (5) |
| Al2–O2 | 1.847 (3) | Al2–O2 | 1.852 (9) | Al4–O4 | 1.85 (1) | Al2–O2 | 1.861 (5) |
| Al2–C3 | 1.966 (4) | Al2–C21 | 1.90 (1) | Al4–C29A | 1.94 (2) | Al2–C3 | 1.960 (7) |
| Al2–C4 | 1.958 (4) | Al2–C25 | 1.96 (1) | Al4–C33A | 1.97 (1) | Al2–C4 | 1.965 (7) |
| | | | Bond Angles | | | | |
| Al1–O1–Al2 | 99.5 (1) | Al1–O1–Al2 | 99.8 (4) | Al3–O3–Al4 | 101.2 (4) | Al1–O1–Al2 | 98.7 (3) |
| Al1–O2–Al2 | 99.2 (1) | Al1–O2–Al2 | 99.6 (4) | Al3–O4–Al4 | 101.2 (4) | Al1–O2–Al2 | 97.3 (2) |
| O1–Al–O2 | 80.6 (1) | O1–Al1–O2 | 80.4 (3) | O3–Al3–O4 | 79.5 (4) | O1–Al1–O2 | 82.2 (2) |
| O1–Al1–C1 | 115.3 (2) | O1–Al1–C29 | 112.5 (6) | O3–Al3–C21A | 114.4 (5) | O1–Al1–C1 | 109.1 (3) |
| O1–Al1–C2 | 112.3 (2) | O1–Al1–C33 | 109.2 (5) | O3–Al3–C25A | 109.8 (5) | O1–Al1–C2 | 115.4 (3) |
| O1–Al2–O2 | 80.6 (1) | O1–Al2–O2 | 80.2 (4) | O3–Al4–O4 | 78.2 (4) | O1–Al2–O2 | 81.8 (2) |
| O1–Al2–C3 | 110.7 (2) | O1–Al2–C21 | 108.8 (5) | O3–Al4–C29A | 114.0 (5) | O1–Al2–C3 | 109.6 (3) |
| O1–Al2–C4 | 112.6 (2) | O1–Al2–C25 | 114.1 (5) | O3–Al4–C33A | 110.8 (5) | O1–Al2–C4 | 112.9 (3) |
| O2–Al1–C1 | 110.1 (2) | O2–Al1–C29 | 108.0 (4) | O4–Al3–C21A | 107.3 (5) | O2–Al1–C1 | 112.6 (3) |
| O2–Al1–C2 | 112.4 (2) | O2–Al1–C33 | 114.6 (4) | O4–Al3–C25A | 118.0 (5) | O2–Al1–C2 | 108.9 (3) |
| O2–Al2–C3 | 115.3 (2) | O2–Al2–C21 | 116.3 (5) | O4–Al4–C29A | 109.6 (5) | O2–Al2–C3 | 111.3 (3) |
| O2–Al2–C4 | 113.8 (2) | O2–Al2–C25 | 108.4 (5) | O4–Al4–C33A | 113.8 (5) | O2–Al2–C4 | 111.1 (3) |
| C1–Al1–C2 | 119.6 (2) | C29–Al1–C33 | 123.9 (6) | C29A–Al4–C33A | 122.2 (6) | C1–Al1–C2 | 121.9 (3) |
| C3–Al2–C4 | 117.9 (2) | C21–Al2–C25 | 121.7 (6) | C21A–Al3–C25A | 120.7 (6) | | |

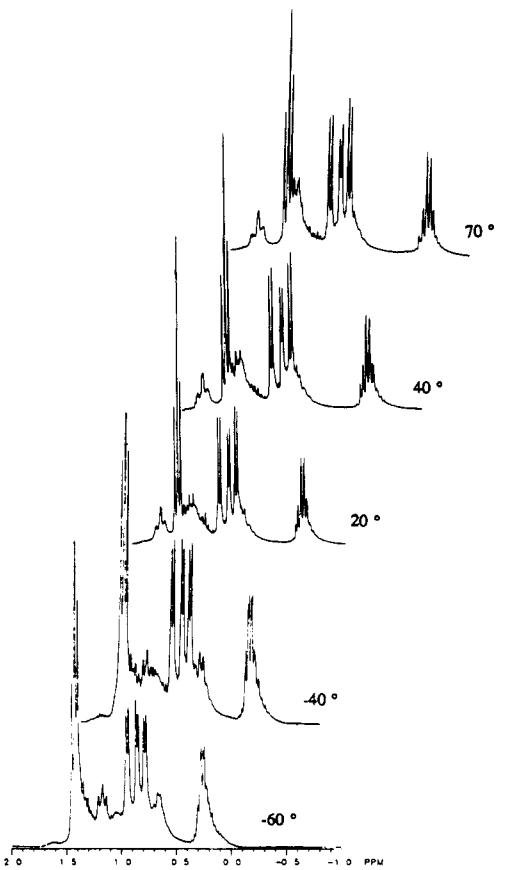


**Figure 4.** $^1H$ NMR spectrum of $[Et_2Al(\mu\text{-}l\text{-mentholate})]_2$ (**1b**) as a function of temperature, showing only the upfield region.

behavior, but the $^1H$ NMR spectrum of $[Et_2Al(\mu\text{-}l\text{-mentholate})]_2$ shows splitting of the methylene protons of the ethyl group, which disappears between 60 and 70 °C (Figure 4). In the isobutyl derivative $[(i\text{-}Bu)_2Al(\mu\text{-}l\text{-mentholate})]_2$ nonequivalence of the methylene protons, of the methyl protons, and of the methyl carbon atoms of

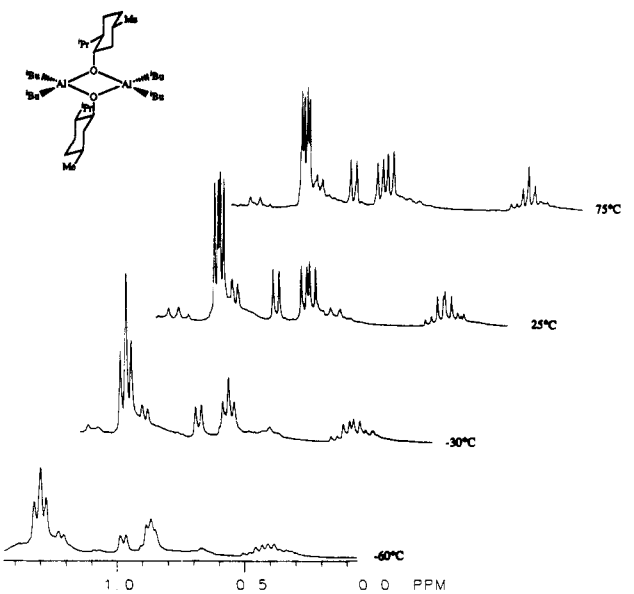


**Figure 5.** $^1H$ NMR spectrum of $[(i\text{-}Bu)_2Al(\mu\text{-}l\text{-mentholate})]_2$ (**1c**) as a function of temperature, showing only the upfield region.

the isobutyl groups is observed. Partial variable-temperature $^1H$ NMR spectra are shown in Figure 5. These spectra show that substantial chemical shift changes occur as a function of temperature, but the lines do not coalesce, implying that the chemical exchange process does not become rapid on the NMR time scale for this derivative, even at 75 °C in toluene solution. Comparable studies on the related borneolates **2a–c** reveal no such behavior. The $^1H$ NMR spectrum of $[(i\text{-}Bu)_2Al(\mu\text{-}l\text{-borneolate})]_2$ is shown in Figure 6.

Two possible explanations for this NMR behavior were considered: first, the optically active center associated with the bridging ligand gave rise to the nonequivalence observed; second, the nonequivalence arose as a result of the steric interaction between the bridging groups and the alkyl substituents bound to the aluminum. The first

**Table IX. Selected Bond Distances (Å) and Angles (deg) in Organoaluminum Alkoxides**

| compd | Al–O | Al–C | Al···Al | C–Al–C | O–Al–O | Al–O–Al | ref |
|---|---|---|---|---|---|---|---|
| $[Me_2Al(\mu\text{-}l\text{-mentholate})]_2$ | 1.841 | 1.963 | 2.807 | 118.7 | 80.6 | 99.4 | this work |
| $[(i\text{-}Bu)_2Al(\mu\text{-}l\text{-mentholate})]_2$ | | | | | | | |
| molecule 1 | 1.839 | 1.956 | 2.823 | 123.3 | 79.8 | 100.2 | this work |
| molecule 2 | 1.842 | 1.942 | 2.840 | 120.7 | 79.1 | 100.9 | this work |
| $[Me_2Al(\mu\text{-}l\text{-borneolate})]_2$ | 1.841 | 1.956 | 2.779 | 122.3 | 82.0 | 98.0 | this work |
| $[Me_2Al(\mu\text{-2-allyl-6-methylphenoxide})]_2$ | 1.861 | 1.946 | 2.866 | 115.4 | 79.2 | 100.8 | 12 |
| $[Me_2Al(\mu\text{-O-}t\text{-Bu})]_2$ (gas) | 1.864 | 1.962 | 2.82 | 121.7 | 81.9 | 98.1 | 16 |
| $Me_3Al$ (gas) | | 1.957 | | | | | 19 |
| $Et_2AlBHT{\cdot}CH_3C_6H_4CO_2Me$ | 1.749 | 1.964 | | 116.4 | 101.7 | | 18 |
| | 1.887 | | | | | | |
| $Me_2AlBHT{\cdot}PMe_3$ | 1.736 | 1.970 | | 111.7 | | | 17 |
| $K[Me_6Al_2(\mu\text{-OPh})\cdot$dibeno-18-crown-6 | 1.891 | 2.008 | | 112.7 | | 127.5 | 20 |
| $K[Me_2Al(OPh)_2]$ | 1.800 | 1.968 | | 119.4 | 96.8 | | 20 |
| $[AsMe_4]_2[Me_2AlOAlMe_3]_2$ | 1.79 | | | | | 96.0 | 21 |
| $[Al_2(OSiMe_3)_4(acac)_2]$ | 1.838 | | | | 86.8 | 97.4 | 22 |
| $[Me_2Al\{\mu\text{-}O(CH_2)_2OMe\}]_2$ | 1.859 | 1.951 | 2.924 | 120.8 | 76.3 | 103.1 | 13 |
| $[Me_2Al\{\mu\text{-}OCH(Me)N(Ph)CH(Ph)O\}]_2$ | 1.922 | 1.964 | | 119.4 | 73.7 | 105.3 | 23 |
| $[Me_2Al\{\mu\text{-}OCH_2\text{-}2\text{-}(C_5H_4N)\}]_2$ | 1.894 | 1.994 | 3.024 | 119.1 | 74.1 | 105.9 | 14 |
| $[Me_2Al\{\mu\text{-}OCH(Ph)CH(Me)N(H)Me\}]_2$ | 1.905 | 1.994 | 3.000 | 118.5 | 74.8 | 104.0 | 24 |

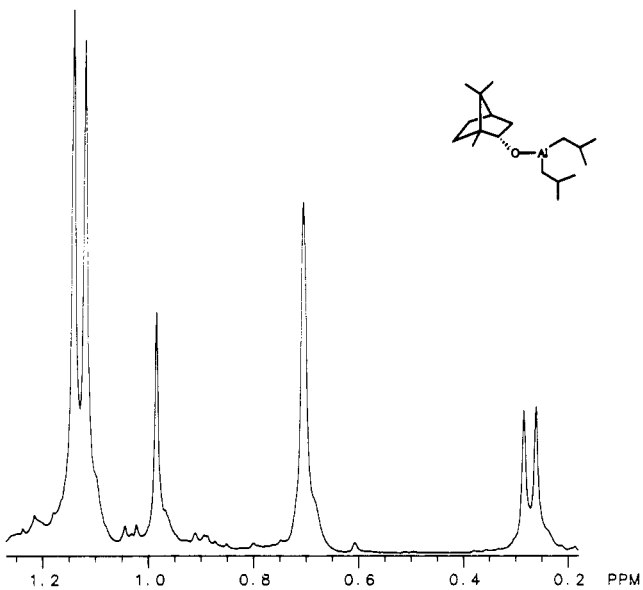


**Figure 6.** $^1H$ NMR spectrum of $[(i\text{-}Bu)_2Al(\mu\text{-}l\text{-borneolate})]_2$ (**2c**) showing only the upfield region.

proposal was rejected on two counts: first, nonequivalence was observed in the *l*-menthol derivatives and not in the *l*-borneol derivatives; second, the nonequivalence appeared to be temperature-dependent. Close examination of the NMR spectral results and structures suggests that the second proposal provides a satisfactory explanation for the observed behavior. We established previously that hindered rotation of alkoxide-bridged organoaluminum compounds leads to nonequivalence of the alkyl groups bound to the aluminum center.[12] Furthermore, it was found that the rate of rotation of the phenoxide around the C–O bond is a function of both the bridging group and of the alkyl group on aluminum. In the present case we have two very different bridging ligands. Figure 4 provides a view of **1a,c** and **2a** which shows that the very rigid *l*-borneolate group is oriented in a way so that it should not interact with any alkyl group bound to aluminum. In the case of the *l*-mentholate derivatives, the isopropyl groups in the 2-position on the *l*-mentholate ring system are oriented so that they may interact substantially with the terminal alkyl groups bound to aluminum. When R = Me in $[R_2Al(\mu\text{-}l\text{-mentholate})]_2$, the steric requirements would be minimal. For R = Et, they would be more pronounced, and hindered rotation could become a factor. Finally, for R = *i*-Bu, they should be maximum. On the basis of the structural data and the temperature dependence of the NMR spectra, it

**Scheme III**

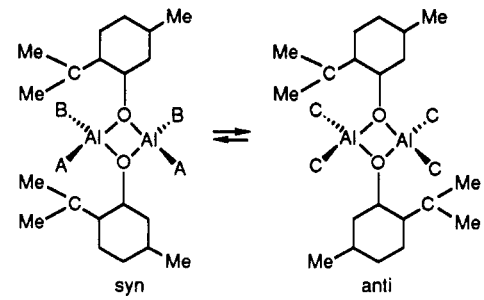


appears that the nonequivalence results from hindered rotation about the bridge and/or about the Al–C bonds. Scheme III provides some additional insight. If one examines the different sites in the syn and anti conformations, it is clear that in the syn conformation two different environments are present, represented by A and B. In the anti conformation a third magnetic environment, C, is present (assuming alkyl groups are free to rotate). If the alkyl groups are not free to rotate, nonequivalence of the protons and carbon atoms on the alkyl chain should be observed. Our observation that $[(i\text{-}Bu)_2Al(\mu\text{-}l\text{-mentholate})]_2$ (**1c**) is in an anti conformation in the solid state (see X-ray Structures) and shows two types of isobutyl groups in solution suggests that the anti conformer has undergone equilibration with the syn conformer in solution or, alternatively, that the isobutyl groups are locked into position, causing the $\gamma$-carbon atom and the proton on the alkyl chain to become nonequivalent. Further, the lack of line broadening and coalescence indicates that the barrier to rotation is relatively high. Careful examination of both the $^1H$ and $^{13}C$ NMR spectra indicate that the isobutyl groups attached to the aluminum are nonequivalent. They do not indicate that there are two types of menthol ligand nor do they indicate three types of isobutyl groups as required by the anti $\rightleftharpoons$ syn equilibrium. This latter behavior is well documented in our earlier observation on $[Me_2Al(\mu\text{-2-allyl-6-methylphenoxide})]_2$, in which the anti conformation was observed in the solid state, but in solution both syn and anti forms were found in nearly equivalent concentrations.[12]

In this case, from the evidence at hand, it appears that the complex remains in the anti conformation with the isobutyl groups locked into their positions, giving rise to nonequivalence of the methylene protons and the $\gamma$-carbon atoms. In $[Et_2Al(\mu\text{-}l\text{-mentholate})]_2$ the ethyl groups also have nonequivalent protons which show temperature-dependent behavior. The data are insufficient to determine

if this results from hindered rotation about the Al–C bond or because of hindered rotation about the O–C bond of the bridging group. In all cases there was no evidence for dissociation of the Al–O–Al bridge bond in solution. Further, in separate experiments, it was shown that THF did not form a stable adduct with **1a** nor did diethyl ether form a stable adduct with **2a**.

**Acknowledgment** is made to the donors of the Petroleum Research Fund, administered by the American Chemical Society, for the support of this research.

**Registry No.** **1a**, 136763-63-8; **1b**, 136763-64-9; **1c**, 136763-65-0; **2a**, 136763-66-1; **2b**, 136763-67-2; **2c**, 136763-68-3; $Me_3Al$, 75-24-1; $Et_3Al$, 97-93-8; $(i\text{-}Bu)_3Al$, 100-99-2; *l*-menthol, 2216-51-5; *l*-borneol, 464-45-9.

**Supplementary Material Available:** Complete listings of bond distances and angles, anisotropic thermal parameters for the non-hydrogen atoms, hydrogen atom coordinates, and isotropic thermal parameters and unit cell packing diagrams for **1a,c** and **2a** (17 pages); listings of observed and calculated structure factors for **1a,c** and **2a** (67 pages). Ordering information is given on any current masthead page.

# Coordination Chemistry of Group 14 Metalloles. 7.[1] Fluxional Behavior of *cis*-MLL'($\eta^4$-metallole)$_2$ (M = Mo, W) Complexes

Geneviève Cerveau, Ernest Colomer,* Hari K. Gupta, and Marc Lheureux

*Laboratoire "Hétérochimie et Aminoacides", URA CNRS 1097, Institut de Chimie Fine, Université de Montpellier II, Place Eugène-Bataillon, F-34095 Montpellier Cedex 5, France*

Adrien Cavé

*Centre CNRS, INSERM de Pharmacologie-Endocrinologie, Rue de la Cardonille, B.P. 5055, F-34033 Montpellier Cedex, France*

*Received June 20, 1991*

Complexes of the type *cis*-MLL'($\eta^4$-metallole)$_2$ exhibit fluxionality in solution. A study by variable-temperature $^1H$, $^{13}C$, and $^{31}P$ NMR allows the determination of factors which govern fluxionality and the mechanisms which explain isomerization. When L = L' = CO, an equilibrium between rotational enantiomers (cis-Δ uu and cis-Λ uu) is observed; in addition, when the metallole is C-unsubstituted or substituted by methyl groups in the 3- and 4-positions, a rotational racemic diastereoisomer is also observed. The interconversion between diastereoisomers is faster than the one between enantiomers for steric reasons. For L = L' = $PMe_3$ or for L = CO and L' = $P(OPh)_3$ (ligands which have, respectively, the same electronic effect but are more sterically demanding than two CO ligands), only an equilibrium between cis-Δ uu and cis-Λ uu enantiomers is present. When the metalloles are phenyl C-substituted, diastereoisomers cannot be detected. These interconversions are well explained by a ring rotation mechanism. A different situation occurs when L and L' are complementary ligands [L = CO; L' = $PPh_3$, $PPh_2Me$, $P(p\text{-tol})_3$]; then the coexistence of cis-Δ uu and trans-ou is observed. The different isomers are detected, namely, by the different coupling constants of the carbonyl signals with the phosphorus nucleus. This equilibrium implies the coexistence of a fast ring rotation mechanism (cis-Δ uu ⇌ cis-Λ uu interconversion) and a slow Bailar twist (cis-Δ uu ⇌ trans-ou interconversion).

## Introduction

We previously described the crystal structure and the dynamic stereochemistry of complexes of the type LL'-bis($\eta^4$-metallole)transition metal[2-4] (L = CO, L' = $PPh_3$). The X-ray study of dicarbonylbis($\eta^4$-1,1,3,4-tetramethylsilole)molybdenum (**7**) (Chart I) revealed that the structure is cis-uu[5] (Chart II). The structures of other related complexes were assumed to be identical by analogy.

In solution, the situation is different, since the IR spectra of these complexes showed the presence of diastereoisomers for all the series. [These isomers are rotamers; however, the terms diastereoisomers and enantiomers are used for more clarity.] Their fluxional behavior was investigated by variable-temperature NMR experiments. Dicarbonyl complexes showed an averaged $^1H$ NMR spectrum at 300 K, but at ~100 K the nonequivalence of the olefinic and of the methyl protons in the 3- and 4-positions was observed (as predicted by the X-ray analysis). Nevertheless, diastereoisomers were not observed with this technique.

The $^1H$ NMR spectrum of carbonylbis($\eta^4$-1,1-dimethylsilole)(triphenylphosphine)molybdenum (**1**) showed four signals for the olefinic protons at 300 K. This is consistent with a fluxional cis complex which isomerizes via a ring rotation mechanism (Figure 1). But, in contrast to that of the dicarbonyl complexes, its low-temperature spectrum showed 12 signals for the olefinic protons and 8 for the methyl ones. This was attributed to a slow equilibrium between the cis-uu and the trans-ou diastereoisomers; indeed, the coexistence of one cis isomer and the trans-ou one was the only one compatible with such multiplicity. This interconversion was explained via an intramolecular nondissociative process; a Bailar twist[8] was invoked as being the most consistent with the $\eta^4$-coordi-

(1) Part 6: Colomer, E.; Corriu, R. J. P.; Lheureux, M. *Butll. Soc. Catalana Cienc.*, in press.
(2) Carré, F.; Colomer, E.; Corriu, R. J. P.; Lheureux, M.; Cavé, A. *J. Organomet. Chem.* **1987**, *331*, 29.
(3) Colomer, E.; Corriu, R. J. P.; Lheureux, M. *Chem. Rev.* **1990**, *90*, 265.
(4) Colomer, E.; Corriu, R. J. P.; Lheureux, M. *Organometallics* **1989**, *8*, 2343.
(5) For nomenclature rules, see refs 6 and 7.
(6) Kreiter, C. G.; Ozkar, S. *J. Organomet. Chem.* **1978**, *152*, C13.
(7) Kreiter, C. G. *Adv. Organomet. Chem.* **1986**, *26*, 297.
(8) Bailar, J. C. *J. Inorg. Nucl. Chem.* **1958**, *8*, 165.

0276-7333/92/2311-0214$03.00/0 